Pharm Res (2014) 31:2107–2123
DOI 10.1007/s11095-014-1312-8

RESEARCH PAPER

Pharmacokinetic Comparison Between the Long-Term Anesthetized, Short-Term Anesthetized and Conscious Rat Models in Nasal Drug Delivery

Yin Cheong Wong • Shuai Qian • Zhong Zuo

Received: 23 August 2013 / Accepted: 16 January 2014 / Published online: 20 February 2014

ABSTRACT

Purpose To investigate the pharmacokinetic differences between the common nasal delivery models.

Methods In three different rat models [long-term anesthetized (with nasal surgery), short-term anesthetized (without nasal surgery) and conscious models], tacrine and loxapine were administered via nasal, intravenous and oral routes, and the plasma pharmacokinetics were compared among different models.

Results Systemic exposures of both drugs and their metabolites were consistently higher in long-term anesthetized model after all routes of administration in comparison to that of conscious model. Nasal bioavailabilities in long-term anesthetized model (tacrine 83%, loxapine 97%) were much higher than that in conscious model (tacrine 10%, loxapine 46%). Further studies on tacrine and its metabolites demonstrated no significant difference in $t_{1/2}$ between short-term anesthetized and conscious models after all routes of administration; however, long-term anesthetized model showed significantly longer $t_{1/2}$. Regarding the pharmacokinetic parameters (C_{max}, T_{max}, AUC, bioavailability) of tacrine and its metabolites, short-term anesthetized model resembled closer to conscious model than long-term anesthetized model.

Conclusions Plasma clearances of tacrine, loxapine, and their metabolites were much slower in the long-term anesthetized model of nasal delivery probably due to suppressed hepatic and renal clearances, while the short-term anesthetized model imposed less impact on tacrine pharmacokinetics and metabolism.

KEY WORDS anesthesia · intranasal administration · laboratory animal models · metabolism · pharmacokinetics

Y. C. Wong • S. Qian • Z. Zuo (✉)
School of Pharmacy, Faculty of Medicine
The Chinese University of Hong Kong
Room 801C, Lo Kwee-Seong Integrated Biomedical Sciences Building
Shatin, New Territories, Hong Kong
e-mail: joanzuo@cuhk.edu.hk

ABBREVIATIONS

1-OH-THA	1-hydroxytacrine
2-OH-THA	2-hydroxytacrine
4-OH-THA	4-hydroxytacrine
7-OH-AMOX	7-hydroxyamoxapine
7-OH-LOX	7-hydroxyloxapine
8-OH-AMOX	8-hydroxyamoxapine
8-OH-LOX	8-hydroxyloxapine
AMOX	Amoxapine
AUC	Area under the curve
CL_{total}	Total systemic clearance
C_{max}	Maximum concentration
CYP	Cytochrome P450
GI	Gastrointestinal
i.n.	Intranasal
i.v.	Intravenous
LOX	Loxapine
p.o.	Oral
PK	Pharmacokinetics
$t_{1/2}$	Elimination half life
THA	Tacrine
T_{max}	Time to reach maximum concentration
V_d	Volume of distribution

INTRODUCTION

Rodents, particularly rats, are the most common laboratory animals used for preclinical pharmacokinetic (PK) evaluation of nasal delivery (1). These animals are usually anesthetized during experiments to facilitate nasal drug administration. In the classic rat model for studying nasal drug absorption described by Hussain *et al.* (2), nasal surgery was conducted to isolate the nasal cavity with the rat being kept anesthetized by a long-acting injectable anesthetic agent such as ketamine (3,4) and pentobarbital (5) throughout the entire period of PK

experiment. It is known that anesthetic agents, particularly the long-acting ones such as ketamine, could dramatically alter the physiological conditions of the animals resulting in modified drug absorption, distribution, metabolism and elimination (6). Therefore, when evaluating the drug bioavailability and PK, the results must be treated with caution if anesthesia has been applied. For instance, the bioavailability of sublingual verapamil in conscious rabbit was 40% while that in ketamine/xylazine anesthetized rabbits was 108% (7). In addition to anesthesia, the nasal surgery might further affect the PK of the nasal drug since surgery, as with other forms of stress, also exerts significant influence on physiological functions (8). For instance, surgery and ketamine/xylazine anesthesia could markedly decrease both cytochrome p450 (CYP) 3A activity and hepatic blood flow in rats (9). Although the classic long-term anesthetized rat model has been adopted in numerous nasal drug absorption studies for more than three decades, it is surprising that there was only one published study that compared the drug PK between the classic rat model and the conscious rats. In that study, Yang *et al.* (10) reported that the systemic clearance of intravenous (i.v.) stavudine was significantly reduced in the classic rat model compared with the conscious rats. However, the PK of intranasal (i.n.) stavudine in the conscious rats was not studied.

In addition to the long-term anesthetized model with nasal surgery, short-term anesthetized model without nasal surgery has also been adopted in several studies to evaluate the nasal drug absorption. Since accurate nasal dosing in conscious rats is difficult to achieve due to moving and escaping during drug administration, inhalation anesthetic agents (e.g. diethyl ether (11), halothane (12), and isoflurane (13)) are employed to induce temporary sedation which facilitates nasal drug administration. Compared with long-term anesthesia, short-term anesthesia causes less impact on the PK of, for example, sublingual (7) and i.v. (14) drugs in rodents. It is reasonable to speculate that short-term anesthesia would also cause less impact on the PK of nasal drugs, although direct PK comparison between the short-term anesthetized, long-term anesthetized and conscious rat models has not been reported.

Although there exists quite a number of reports on the effects of anesthetic agents on the PK of xenobiotics after non-nasal route of administration, in most cases only the PK of parent drugs were measured. This could result in wrong conclusion if the effects of anesthesia on the formation and disposition of metabolites are not analyzed (15). For nasal drug delivery, studying the metabolite formation could provide valuable information on, for example, whether the drug is efficiently absorbed within the nasal cavity into systemic circulation or is swallowed into gastrointestinal (GI) tract with subsequent first-pass metabolism (readers are referred to our previous review (16)). However, the drug metabolites were not investigated in most literature reports on nasal delivery even though many of the metabolites have prominent contribution to the clinical effects of the drugs (17).

Loxapine (LOX) and tacrine (THA) are selected as model compounds in the present study. Both of them are small, lipophilic drugs that have demonstrated satisfactory permeability (in the order of 10^{-5} cm/s) across the Calu-3 monolayer (18,19), an *in vitro* model of respiratory epithelium for screening of compounds for potential nasal drug delivery (20). LOX is a highly extracted drug (with hepatic extraction ratio in humans of 0.71) (21) which is almost completely metabolized after oral administration to rats (22). THA is also highly extracted by the rat liver with a hepatic extraction ratio of up to 70 to 100% (23). Our preliminary PK studies demonstrated that LOX (22) and THA (24) are extensively metabolized in rats to phase I active metabolites (Fig. 1), making them suitable for investigation of the differences in drug metabolism between the rat models. Yet, the CYPs involved in the metabolism of LOX and THA are different (Fig. 1), which allows us to elucidate the effect of anesthesia on different CYP-mediated metabolic pathways. In brief, THA is classified by FDA as an acceptable *in vitro* substrate and a sensitive *in vivo* substrate for CYP 1A2 studies. LOX, on the other hand, is predominantly metabolized in rats by CYP 3A and CYP 2D to two primary metabolites amoxapine and 7-hydroxyloxapine, which are further metabolized to a secondary metabolite 7-hydroxyamoxapine (22,25). Both LOX and THA are eliminated from the rat mainly as these metabolites in the urine (26,27).

The objectives of the present study are to: 1) Explore the PK difference between the long-term anesthetized model and conscious model of nasal delivery; and 2) Investigate the feasibility of using the short-term anesthetized model as an alternative model in nasal delivery study. In addition to the nasal route, the PK of LOX and THA after i.v. and oral (p.o.) routes of drug administration were also investigated to elucidate whether the differences between different rat models are route-dependent. To achieve the first research objective, we compared the plasma PK parameters of LOX between the long-term anesthetized model and conscious model after i.n., i.v. and p.o. LOX administration, which served as a "proof-of-concept" trial. To achieve the second research objective, further investigations were performed to compare the PK of THA between the long-term anesthetized, short-term anesthetized and conscious models, aiming to confirm the findings from LOX and also to investigate whether the short-term anesthetized model could be a better alternative of the long-term anesthetized model for PK investigations. In addition to the parent drugs, the phase I metabolites of LOX (22) and THA (24) in plasma were also measured by sensitive, validated HPLC methods, which would help to elucidate the metabolic differences between different rat models.

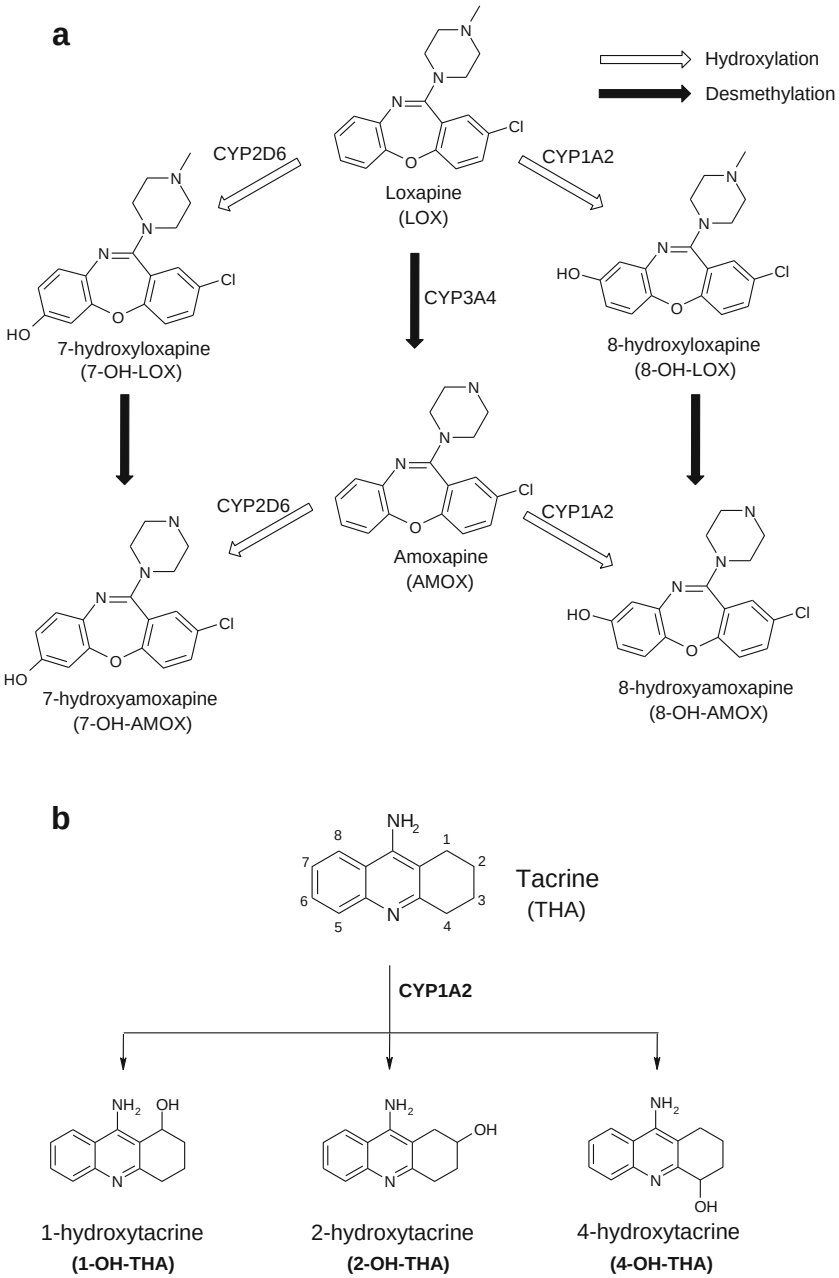

Fig. 1 Summary of metabolic pathways of (**a**) loxapine and (**b**) tacrine and the major CYPs involved.

MATERIALS AND METHODS

Materials

LOX succinate and amoxapine (AMOX) were obtained from Sigma (St. Louis, MO, USA). 7-hydroxyloxapine (7-OH-LOX), 8-hydroxyloxapine (8-OH-LOX), 7-hydroxyamoxapine (7-OH-AMOX) and 8-hydroxyamoxapine (8-OH-AMOX) were purchased from TC Scientific Inc. (Alberta, Canada). THA hydrochloride was purchased from Enzo Life Sciences Inc. (Farmingdale, NY, USA). 1-hydroxytacrine (1-OH-THA), 2-hydroxytacrine (2-OH-THA) and 4-hydroxytacrine (4-OH-THA) were kindly gifted from Pfizer Inc. (Groton, CT, USA). Ketamine (10% injection) and xylazine (2% injection) were obtained from Alfasan International B.V. (Woerden, Holland). All other reagents were of at least analytical grade and were used without further purification. Distilled and deionized water was used for the preparation of solutions. LOX and THA solutions for administration were prepared by dissolving the compounds in normal saline.

Rat Models and Drug Administration

In the first part of the study, the plasma PK profiles of LOX as well as its metabolites were studied in the long-term

anesthetized model and conscious model after i.v., i.n. and p.o. administration of LOX. In order to confirm the findings from the LOX study and to extend the investigation to the short-term anesthetized model, the plasma PK of THA and its metabolites were then investigated in the long-term anesthetized, short-term anesthetized and conscious models after i.v., i.n. and p.o. administration of THA in the second part of the study.

Male Wistar rats (170–230 g for LOX studies) and Sprague–Dawley rats (230–250 g for THA studies) were provided by Laboratory Animal Services Center of The Chinese University of Hong Kong (Hong Kong, China). Animals were housed in standard cages on 12 h light–dark cycles, fed with standard animal chow and tap water daily. The rats were fasted over night before administration of LOX or THA. All experimental procedures were approved by the Department of Health of Hong Kong and Animal Ethics Committee at the Chinese University of Hong Kong. Surgical procedure and drug administration in the three rat models were described below, and the experimental conditions for each group of rats are summarized in Table I.

Conscious Model

For all the three administration groups (i.v., i.n. and p.o.) in the conscious model, jugular vein catheterization was performed 1 day before the PK experiment. Briefly, the right jugular vein of rat was catheterized with a polyethylene tubing (0.5 mm I.D., 1 mm O.D., Portex Ltd., England) under anesthesia induced by intramuscular injection of a mixture containing ketamine (80 mg/kg) and xylazine (8 mg/kg). The polyethylene tube was led under the skin and exteriorized at the back of the neck for blood sampling. 50 I.U./ml of heparin sodium in normal saline was filled into the catheter to prevent blood clotting. After the exposed areas were sutured, the rats were placed individually in standard cages, and they were allowed to recover for 24 h before drug administration.

For i.v. administration, 0.3 ml of LOX or THA solution (equivalent to 0.3 mg/kg and 4 mg/kg, respectively) was injected through the catheter, followed by injection of 0.5 ml of blank rat blood (withdrawn from the same rat just before drug injection) and then 0.5 ml of heparinized normal saline (25 I.U./ml) to rinse the residual drug remained in the catheter. For i.n. administration, rats were hand-restrained and placed in an upright position with the head in the vertical position. 20 μl of LOX or THA solution (equivalent to 0.3 mg/kg and 4 mg/kg, respectively) was administered by micropipette in drops, alternating between each naris within 2 min (10 μl for each nostril) (28). The drops were placed onto the naris and naturally sniffed in by the rats. For p.o. administrations, 1 ml of LOX or THA solution (equivalent to 0.3 mg/kg and 4 mg/kg, respectively) was gavaged to rats. After the above dosing, the conscious rats were returned to cage with free access to water.

Long-Term Anesthetized Model

In the long-term anesthetized model, all rats received intramuscular ketamine/xylazine (80/8 mg/kg) injection to induce anesthesia on the day of experiment. Rats in p.o. group received jugular vein catheterization 24 h before drug administration as that in the conscious model, while rats in i.v. and i.n. groups received the catheterization procedures immediately before drug administration. For i.n. group, additional nasal surgery was conducted immediately before drug administration according to the method described by Hussain *et al.* (2). Briefly, the rat was placed in supine position. An incision (~1 cm) was made on the neck at 1.5 cm from lower lip, and the trachea was cannulated with a polyethylene hollow tube (1.5 mm I.D., 3.1 mm O.D.) to aid breathing. Another sealed polyethylene tube (2.0 mm O.D.) was inserted from the esophagus to the posterior part of the nasal cavity to prevent any drainage of drug solution from nasal cavity to the posterior part of oral cavity or to GI tract. The nasopalatine was sealed with an adhesive agent to prevent drainage of the drug solution from nasal cavity to the anterior part of oral cavity.

For i.v. administration, the right jugular vein was catheterized under ketamine/xylazine induced long-term anesthesia, followed by injection of 0.3 ml of LOX or THA solution (equivalent to 1 mg/kg and 4 mg/kg, respectively) via the catheter. For i.n. administration, the anesthetized rats were placed in supine position, and 20 μl of LOX or THA solution (equivalent to 1 mg/kg and 4 mg/kg, respectively) was administered via a cannula (polythene tube, 0.5 mm I.D., 1.0 mm O.D.) inserted 5 mm into the nasal cavity of naris. For p.o. administration, the awake rats were first gavaged with 1 ml of LOX or THA solution (equivalent to 1 mg/kg and 4 mg/kg, respectively), followed by ketamine/xylazine (80/8 mg/kg) intramuscular injection to induce anesthesia immediately.

For all rats in the long-term anesthetized model, subsequent doses of ketamine (33 mg/kg) and xylazine (3.3 mg/kg) were injected intramuscularly every 90 min to maintain anesthesia, and the body temperature was maintained by a heating lamp throughout the study period.

Short-Term Anesthetized Model

In the short-term anesthetized model, rats in all three administration groups received jugular vein catheterization 24 h before drug administration as described above. No nasal surgery was performed in any group.

Before drug administration, rats were placed in a covered glass cylinder jar (8 in. × 7 in., height × I.D.) which contained a gauze sponge saturated with diethyl ether (60 ml). Each rat

Table I Comparison of Experimental Conditions of the Conscious, Long-Term Anesthetized and Short-Term Anesthetized Rat Models

Rat model	LOX dose (mg/kg)	THA dose (mg/kg)	Anesthetic applied during drug dosing	Nasal surgery	Jugular vein catheterization	Drug administration		Anesthesia maintained
						Route	Position during/after dosing	
Conscious	0.3	4	no	no	A	i.v. i.n.	normal/normal upright/normal	no
						p.o.	upright/normal	
Long-term anesthetized	1	4	ketamine/xylazine	no yes	B B	i.v. i.n.	supine/supine supine/supine	by repeated ketamine/xylazine
				no	A	p.o.	upright/supine	
Short-term anesthetized	N.A.	4	diethyl ether	no	A	i.v. i.n.	supine/normal supine/normal	no
						p.o.	upright/normal	

A: performed 24 h before dosing; B: performed immediately before dosing; N.A.: not applicable

remained in the jar for 3 min. The rats took an average time of 5.2 min (s.d. 1.5 min, $n=10$) to recover from anesthesia (with obvious struggling to right themselves).

For i.v. administration, 0.3 ml of THA solution (equivalent to 4 mg/kg THA) was injected following the same procedure described above for the conscious rats. For i.n. administration, the rats were placed in supine position and 20 μl of THA solution (10 μl for each nostril, equivalent to 4 mg/kg THA) was administered via a cannula (polythene tube, 0.5 mm I.D., 1.0 mm O.D.) inserted 5 mm into the nasal cavity of naris. For p.o. group, 1 ml of THA solution (equivalent to 4 mg/kg THA) was gavaged to the slightly recovered rats (around 5 min after diethyl ether anesthesia). After the above dosing, the rats were returned to cage with free access to water.

Sample and Data Analyses

After drug administration, around 200 μl of blood was collected via the jugular vein catheter into a heparinized centrifuge tube at pre-determined time points. For LOX study, blood was sampled at 3, 5, 10, 15, 20, 30, 45, 60, 120, and 240 min. For THA study, blood was sampled at 2, 5, 10, 15, 20, 30, 45, 60, 90, 120, 180, 240, and 360 min for i.v. group and at 5, 10, 20, 30, 45, 60, 90, 120, 180, 240, and 360 min for i.n. and p.o. groups. After each blood sampling, an equal volume of heparinized normal saline (25 I.U./ml) was injected immediately to the rat via the catheter to flush the catheter and to prevent blood clotting. Plasma samples were obtained by centrifugation of blood at 16,000×*g* for 5 min and were frozen at −80°C until analysis. The analyses of LOX, THA and their metabolites in rat plasma were carried out using our developed and validated LC–MS/MS (22) and HPLC–FLD assays (24), respectively. The lower limits of quantification of the LC-MS/MS assay were 1 ng/ml for LOX and AMOX and 2 ng/ml for the four hydroxylated LOX metabolites. The lower limits of quantification of the HPLC-FLD assay for THA, 1-OH-THA, 2-OH-THA and 4-OH-THA were 2.5, 6.7, 2.1 and 2.1 ng/ml, respectively.

PK parameters were calculated using WinNonlin software (Pharsight Corp., Version 2.1, Mountain View, CA) employing a non-compartmental model approach. The maximum plasma concentration (C_{max}) and the time to reach C_{max} (T_{max}) were directly obtained from plasma data. The terminal half-life ($t_{1/2}$) was calculated as $\ln 2/\lambda_z$, where λ_z was the first-order rate constant associated with the terminal (log-linear) portion of the curve. The area under the plasma concentration-time curve from time 0 to t (AUC_{0-t}) and from time 0 to infinity ($AUC_{0-\infty}$) were calculated by the trapezoidal rule without or with extrapolation to time infinity ($AUC_{0-\infty} = AUC_{0-t} + C_t/\lambda_z$). Bioavailability (F) was calculated as the ratio of $AUC_{0-\infty}$ after i.n. (or p.o.) and i.v. drug administration within the same anesthesia model. Total systemic clearance (CL_{total}) was calculated by dose/$AUC_{0-\infty}$. Volume of distribution (V_d) was calculated by $CL_{total} \times$ mean residence time. Metabolic ratio was calculated by dividing the AUC_{0-t} of the metabolite by the AUC_{0-t} of the parent drug (29). Statistical data analyses were performed using Student's *t*-test or one-way analysis of variance (ANOVA), with $p<0.05$ as the criterion of significance.

RESULTS

PK Comparison between the Conscious and Long-Term Anesthetized Rat Models

LOX and Its Metabolites

The plasma PK profiles of LOX and its metabolites in the conscious and long-term anesthetized models are shown in Fig. 2a and b, respectively. The PK parameters obtained from the two models are compared in Table II. LOX and its

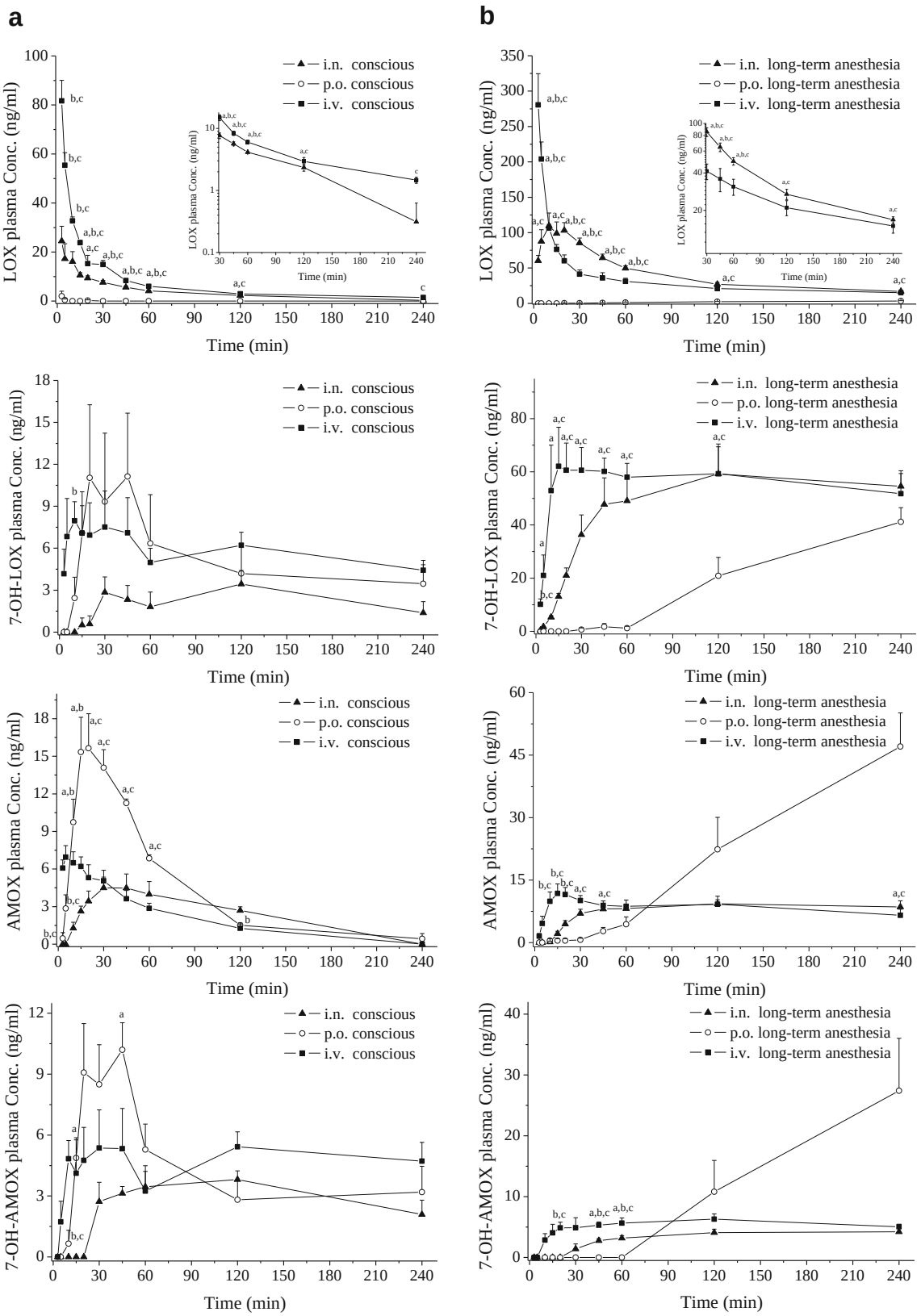

Fig. 2 Plasma pharmacokinetic profiles of LOX and its metabolites after LOX administration via intranasal (i.n.), oral (p.o.) and intravenous (i.v.) routes to (**a**) the conscious model (0.3 mg/kg) and (**b**) the long-term anesthetized models (1 mg/kg). Each point represents mean ± s.d. ($n = 4$). [a] $p < 0.05$ for i.n. *vs* p.o. [b] $p < 0.05$ for i.n. *vs* i.v. [c] $p < 0.05$ for i.v. *vs* p.o.

Table II Comparison of Plasma Pharmacokinetic Parameters of LOX and Its Metabolites Between the Conscious and Long-Term Anesthetized Models After LOX Administration Via i.v., i.n. and p.o. Routes

Pharmacokinetic parameters	i.v.		i.n.		p.o. [e]	
	Conscious	Long-term anesthetized	Conscious	Long-term anesthetized	Conscious	Long-term anesthetized
LOX						
$AUC_{0-\infty}$/dose (min/ml × 10^3)	34.1 ± 3.0	61.5 ± 6.3[b]	15.8 ± 1.9[c]	59.4 ± 4.4[a]	~0	2.3 ± 0.5
F (%)	N.A.	N.A.	46.5	96.6	~0	5.6
T_{max} (min)	N.A.	N.A.	4.8 ± 1.8[c]	15.0 ± 2.9[a,d]	N.A.	≥240
$t_{1/2}$ (min)	81.5 ± 5.3	184.0 ± 16.2[b]	67.0 ± 12.5	99.4 ± 6.2[d]	N.A.	N.A.
CL_{total} (ml/min/kg)	150.0 ± 12.6	84.2 ± 9.6[b]	N.A.	N.A.	N.A.	N.A.
V_d (L/kg)	10.8 ± 0.6	17.7 ± 2.2[b]	N.A.	N.A.	N.A.	N.A.
LOX metabolites[f]						
$AUC_{7\text{-OH-LOX}}$/dose (min/ml × 10^3)	22.5 ± 3.3	66.9 ± 9.2[b]	8.8 ± 2.8[c]	59.3 ± 9.6[a]	20.3 ± 9.1	22.1 ± 4.4
$AUC_{7\text{-OH-LOX}}/AUC_{total}$ (%)	27.7 ± 1.7	53.1 ± 4.3[b]	19.4 ± 5.7	48.6 ± 3.2[a]	32.9 ± 9.2	35.4 ± 2.1
AUC_{AMOX}/dose (min/ml × 10^3)	8.0 ± 1.5	10.1 ± 1.7	9.4 ± 1.6	9.6 ± 1.1	16.2 ± 0.6	25.3 ± 5.4
AUC_{AMOX}/AUC_{total} (%)	9.6 ± 1.1	7.9 ± 0.9	21.6 ± 3.8[c]	8.3 ± 1.2[a]	35.1 ± 8.0	40.3 ± 1.0
$AUC_{7\text{-OH-AMOX}}$/dose (min/ml × 10^3)	18.5 ± 2.0	6.5 ± 0.8[b]	11.3 ± 1.0[c]	4.0 ± 0.5[a,d]	16.3 ± 2.8	13.1 ± 4.5
$AUC_{7\text{-OH-AMOX}}/AUC_{total}$ (%)	23.1 ± 1.1	5.2 ± 0.5[b]	26.0 ± 2.7	3.5 ± 0.7[a]	31.6 ± 4.4	19.9 ± 2.9
AUC_{total}/dose (min/ml × 10^3)	80.0 ± 8.1	125.2 ± 10.1[b]	43.9 ± 3.2[c]	120.1 ± 11.3[a]	52.9 ± 10.7	62.8 ± 13.4
Metabolic ratio						
7-OH-LOX	0.72 ± 0.10	1.69 ± 0.33	0.60 ± 0.18	1.25 ± 0.13[a]	N.A.	12.3 ± 5.4
AMOX	0.25 ± 0.05	0.24 ± 0.04	0.65 ± 0.11[c]	0.21 ± 0.03[a]	N.A.	14.4 ± 6.8
7-OH-AMOX	0.60 ± 0.08	0.16 ± 0.02[b]	0.79 ± 0.08	0.09 ± 0.02[a,d]	N.A.	8.2 ± 4.9
Overall	1.6 ± 0.2	2.1 ± 0.4	2.0 ± 0.1	1.5 ± 0.1[a]	N.A.	34.9 ± 17.1

Data are presented as the mean ± s.d. ($n = 4$)

N.A. not applicable

[a] $p < 0.05$ for comparison between the conscious and anesthetized models in i.n. group

[b] $p < 0.05$ for comparison between the conscious and anesthetized models in i.v. group

[c] $p < 0.05$ for comparison between i.n. group and i.v. group in the conscious model

[d] $p < 0.05$ for comparison between i.n. group and i.v. group in the anesthetized model

[e] In p.o. group, AUC values referred to AUC_{0-4h} since $AUC_{0-\infty}$ could not be calculated, and the plasma concentration of LOX was only quantifiable in one rat in the conscious model

[f] AUC_{total} is the sum of the AUC_{0-4h} of LOX, 7-OH-LOX, AMO and 7-OH-AMO (no 8-OH-loxapine or 8-OH-amoxapine was present in plasma).

metabolites 7-OH-LOX, AMOX and 7-OH-AMOX were present in quantifiable amounts in plasma, while 8-OH-LOX and 8-OH-AMOX were not present in any plasma sample.

i.v. LOX. Compared with the conscious model, CL_{total} of LOX was almost halved in the long-term anesthetized model while $t_{1/2}$ and $AUC_{0-\infty}$ were doubled. Total systemic exposure of LOX and its metabolites (AUC_{total}/dose) was also significantly higher in the long-term anesthetized model. The percentage of LOX converted to 7-OH-AMOX was tremendously reduced while that to 7-OH-LOX was doubled in the long-term anesthetized model.

i.n. LOX. Consistent with the results of the i.v. group, accumulation of LOX and its metabolites were also observed in the long-term anesthetized model of the i.n. group with significant reduction in CL_{total} and V_d of LOX. Regarding the LOX metabolites, the trends of i.n. LOX were also very similar to that of i.v. LOX. Total systemic exposure of LOX and its metabolites was tripled in the long-term anesthetized model while 7-OH-LOX became the dominant metabolite with a concomitant decrease in 7-OH-AMOX formation.

In the long-term anesthetized model, the PK parameters of LOX and its metabolites after i.n. LOX administration were very similar to that of i.v. administration, and the i.n. bioavailability reached 97%. This suggested that i.n. LOX was completely absorbed from the nasal cavity. In the conscious model, the overall metabolic ratio of i.n. LOX (2.0) was not significantly different from that of i.v. LOX (1.6). This might indicate that the portion of the LOX nasal solution swallowed into GI tract (subjected to first-pass metabolism) was minimal in the conscious rats.

p.o. LOX. Trace amount of parent LOX (<5 ng/ml) was found 20 min after p.o. LOX administration in the long-term anesthetized model while the level of LOX was unquantifiable (<1 ng/ml) in most plasma samples in the conscious model. While LOX metabolites appeared in plasma soon after p.o. LOX administration (<3–10 min) in the conscious model, they were not detected until 30 to 60 min in the long-term anesthetized model. Moreover, the plasma levels of the metabolites kept increasing throughout the whole experimental period. This indicated that the ketamine/xylazine anesthesia-induced delay in p.o. absorption was so severe that the absorption of LOX in GI tract had not finished yet, which prevented accurate determination of the PK parameters of LOX metabolites in the long-term anesthetized model. The mechanism leading to the delayed and/or decreased absorption of p.o. LOX in the long-term anesthetized model is multifaceted. First, ketamine (100 mg/kg) was found to lower both the rates of gastric emptying and small intestine transit by 25% at 30 min after ketamine administration to rats (30). Xylazine (3 mg/kg) could also lower the rate of small intestine transit by 70% at 50 min after xylazine administration to mice (31). Second, ketamine/xylazine anesthesia has also been reported to reduce passive permeability of intestinal membrane (32) and intestinal lymphatic absorption and transport of lipophilic compounds (33). The rate of midazolam absorption from the intestinal lumen into the portal vein was also found to be lowered in rats receiving ketamine/xylazine and surgical operation (9). Consequently, both the processes of GI transit of the p.o. LOX dose to the small intestine and the intestinal absorption of LOX into systemic circulation were delayed, which in turn postponed the formation of all the LOX metabolites. On the other hand, since the drug was retained longer in the GI tract, the extent of intestinal metabolism might increase. CYPs 1A, 2B and 3A but not CYP 2D are expressed in rat small intestine (with CYP 3A being the most abundant) and they are enzymatically active (34). Therefore, intestinal metabolism might have contributed to the formation of AMOX by CYP 3A and 1-OH-THA and 2-OH-THA by CYP 1A after p.o. administration, particularly in the long-term anesthetized model.

The dose of LOX applied to the conscious model was lower than that applied to the long-term anesthetized model in order to limit the volume of nasal solution applied to conscious rats, which could help minimize the amount of solution swallowed into GI tract. Both doses were relatively low (0.3 mg/kg in conscious rats and 1 mg/kg in anesthetized rats, equivalent to 2.9 mg and 9.7 mg in a 60 kg human adult (35), respectively). In humans, LOX demonstrated dose-proportional PKs across doses at least between 0.625 and 10 mg (36). Therefore, the apparent discrepancies in PK profiles between the conscious and the anesthetized models should not be attributed to the difference in LOX dose. Moreover, after p.o. administration of 1 mg/kg LOX to conscious (22) or anesthetized rats, almost all LOX was rapidly metabolized to metabolites, leaving trace amount of parent LOX in plasma. This further suggests that saturation of LOX metabolism is not expected under the current LOX doses.

THA and Its Metabolites

The plasma PK profiles of THA and its metabolites in the conscious and long-term anesthetized models after i.v., i.n. and p.o. THA administrations are shown in Figs. 3, 4, and 5, respectively. The PK parameters obtained from the two models are compared in Table III. THA and its metabolites 1-OH-THA and 2-OH-THA were present in quantifiable amounts in plasma, while the concentration of 4-OH-THA was very low and below the limit of quantification in most plasma samples.

i.v. THA. For the parent drug THA, plasma levels in the long-term anesthetized model were higher than that in the conscious model at 4 h and 6 h (enlarged figure of Fig. 3a). The long-term anesthetized model showed a significantly longer $t_{1/2}$ than that of the conscious model (Table III).

Similar to that observed in parent drug, the elimination of the metabolites (1-OH-THA, Fig. 3b; 2-OH-THA, Fig. 3c) was also much slower in the long-term anesthetized model than that in the conscious model. The long-term anesthetized model demonstrated a higher accumulation of metabolites (with much higher $AUC_{0\text{-}6h}$ of both 1-OH-THA and 2-OH-THA as well as higher metabolic ratios, Table III) than that of the conscious model.

i.n. THA. For the parent drug THA (Fig. 4a), a 3.6-fold and 10.3-fold higher C_{max} and $AUC_{0\text{-}6h}$ were obtained in the long-term anesthetized model than the conscious model, respectively (Table III). In addition, the appearance of C_{max} was retarded (T_{max} of 1.3 h) and the elimination of THA was slower ($t_{1/2}$ of 3.2 h) in the long-term anesthetized model when compared with the conscious model (T_{max} of 0.4 h and $t_{1/2}$ of 1.1 h). This is consistent with the delay in T_{max} of i.n. LOX in the long-term anesthetized model (from 4.8 min in the conscious model to 15 min), suggesting that the nasal absorption rate might indeed be reduced in the long-term anesthetized model.

The plasma levels of the two THA metabolites in the long-term anesthetized model remained 2–10 folds higher than that in the conscious model from 1 h till the last sampling time (6 h).

p.o. THA. After p.o. THA administration, the long-term anesthetized model had significantly higher systemic exposures and slower elimination phases of both THA (Fig. 5a) and its metabolites (Figs. 5b and c) than that of the conscious model. The long-term anesthetized model obtained a ~2-fold higher

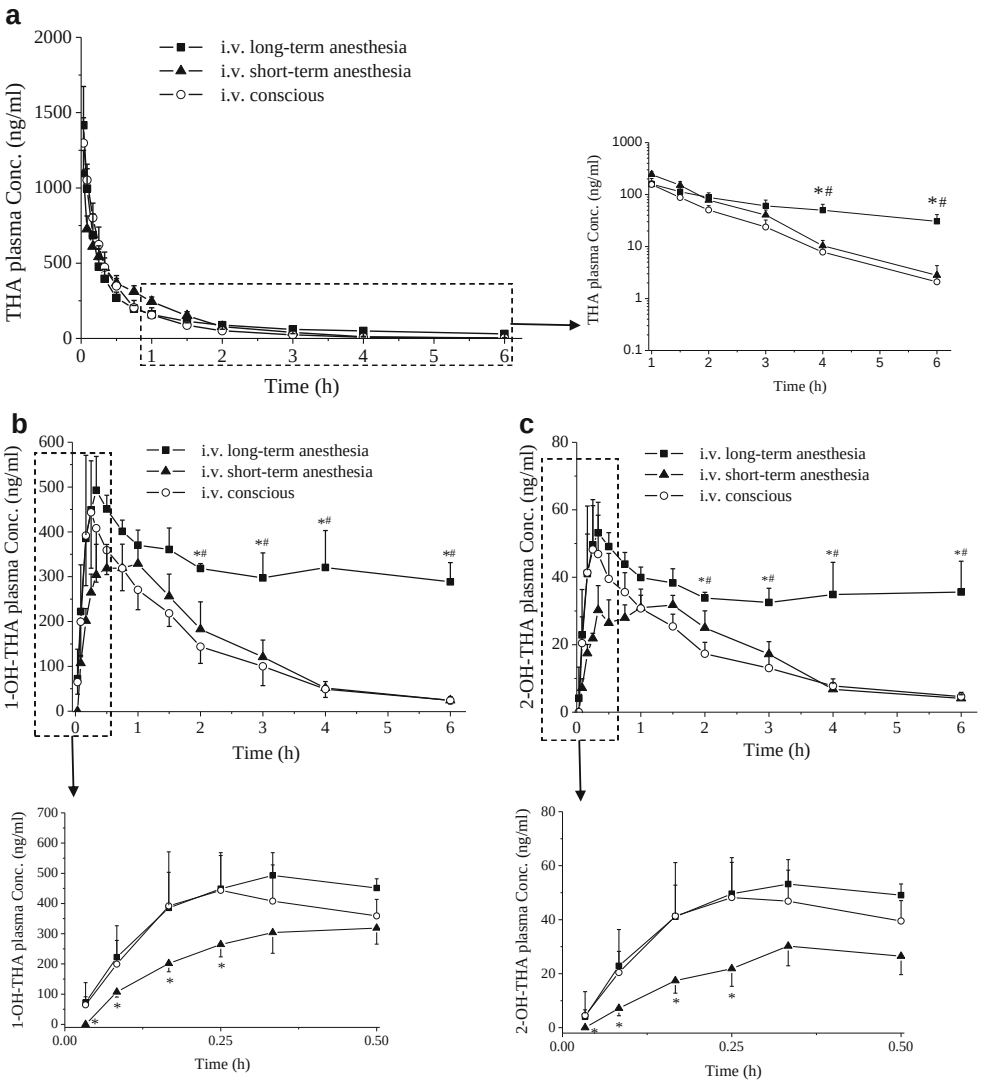

Fig. 3 Plasma pharmacokinetic profiles of (**a**) THA, (**b**) 1-OH-THA and (**c**) 2-OH-THA after i.v. THA administration (4 mg/kg) in the long-term anesthetized, short-term anesthetized and conscious models. Each point represents mean ± s.d. ($n=5$). Certain time periods are enlarged for clarification. * $p<0.05$ for comparison with the conscious model. # $p<0.05$ for comparison with the short-term anesthetized model.

$AUC_{0\text{-}6h}$ of both THA and its metabolites than that of the conscious model (Table III).

For most of the nasal studies adopting the classic long-term anesthetized model, the duration of the PK measurement was limited to 4 (2,37) to 6 h (38,39). The durations of the present studies were therefore set to 6 h for THA and 4 h for LOX. The rationale is that the stresses caused by repeated injections of anesthetic agent (to maintain anesthesia) and nasal surgery would build up and induce progressive changes in physiological functions such as cardiovascular depression (which will be discussed in the Discussion) and respiratory depression (40), and the quality of the obtained PK data might deteriorate after an extended period of time. We acknowledge the limitation that for certain metabolites a complete PK time profile could not be obtained by the end of our experiments, which was particularly obvious for the long-term anesthetized rats. In these rats, at the last sampling time point, the plasma concentration of the parent drug had dropped to a low level while the concentrations of the metabolites remained relatively high, leading to underestimation of the "true" AUC values of the metabolites. Taking this into account, the "true" metabolic ratios in the long-term anesthetized model should be higher than the present values, and the differences in metabolic ratio between the long-term anesthetized model and the other models should be more (statistically) significant.

Feasibility of Using Short-Term Anesthetized Rat Model in Nasal Delivery Study

The plasma PK profiles of THA and its metabolites in the short-term anesthetized model after i.v., i.n. and p.o. THA administrations are shown in Fig. 3, 4 and 5, respectively, with calculated PK parameters shown in Table III. The PK of THA obtained with the short-term anesthetized model are compared to that with the other two models as follows.

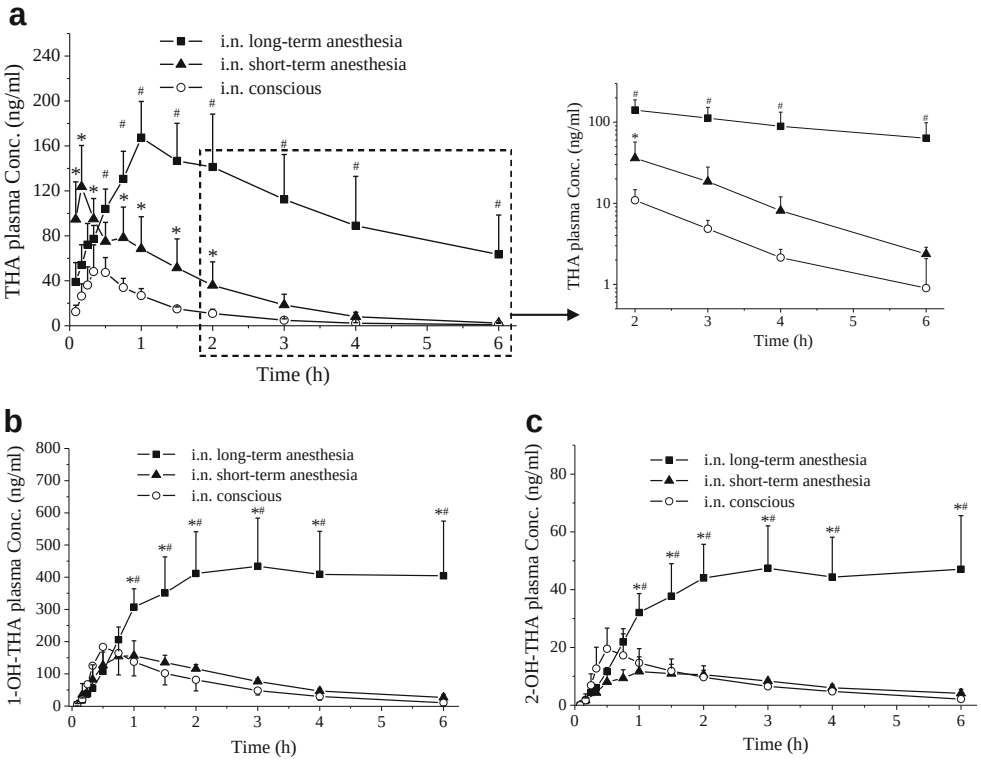

Fig. 4 Plasma pharmacokinetic profiles of (**a**) THA, (**b**) 1-OH-THA and (**c**) 2-OH-THA after i.n. THA administration (4 mg/kg) in the long-term anesthetized, short-term anesthetized and conscious models. Each point represents mean ± s.d. ($n=5$). * $p<0.05$ for comparison with the conscious model. # $p<0.05$ for comparison with the short-term anesthetized model.

i.v. THA

According to ANOVA analysis with multiple comparisons, there was no significant difference in the $t_{1/2}$ of THA between the short-term anesthetized model and conscious model, whereas the long-term anesthetized model showed a significantly longer $t_{1/2}$ than that of the other two models (Table III). In addition, the elimination of the metabolites (1-OH-THA, Fig. 3b; 2-OH-THA, Fig. 3c) was also much slower in the long-term

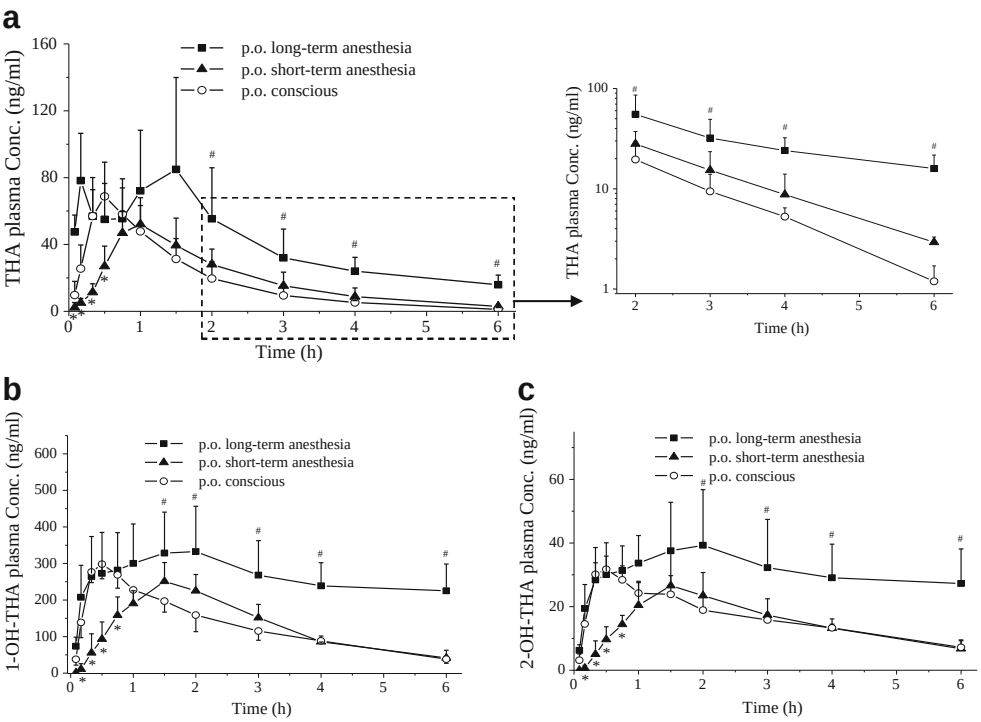

Fig. 5 Plasma pharmacokinetic profiles of (**a**) THA, (**b**) 1-OH-THA and (**c**) 2-OH-THA after p.o. THA administration (4 mg/kg) in the long-term anesthetized, short-term anesthetized and conscious models. Each point represents mean ± s.d. ($n=5$). * $p<0.05$ for comparison with the conscious model. # $p<0.05$ for comparison with the short-term anesthetized model.

Table III Comparison of Plasma Pharmacokinetic Parameters of THA and Its Metabolites Between the Conscious, Long-Term Anesthetized and Short-Term Anesthetized Models After THA Administration Via i.v., i.n. and p.o. Routes

Pharmacokinetic parameters	i.v.			i.n.			p.o.		
	Conscious	Long-term anesthetized	Short-term anesthetized	Conscious	Long-term anesthetized	Short-term anesthetized	Conscious	Long-term anesthetized	Short-term anesthetized
THA									
T_{max} (h)	N.A.	N.A.	N.A.	0.4 ± 0.1	1.3 ± 0.4	0.3 ± 0.3	0.5 ± 0.2	0.8 ± 0.3	1.0 ± 0.3*
C_{max} (ng/ml)	1496 ± 254	1800 ± 439	1092 ± 156	50 ± 20	179 ± 27*#	137 ± 66*#	72 ± 19	98 ± 48	63 ± 14
AUC_{0-6h} (ng·h/ml)	628 ± 101	756 ± 126	711 ± 70	61 ± 16	630 ± 206*#	182 ± 60*#	109 ± 29	217 ± 114*	112 ± 28
$AUC_{0-\infty}$ (ng·h/ml)	631 ± 102	901 ± 171*	716 ± 73	63 ± 15	755 ± 371*#	186 ± 60.*#	112 ± 28	270 ± 118*	118 ± 26
$t_{1/2}$ (h)	0.8 ± 0.2	3.2 ± 1.2*	0.9 ± 0.2	1.1 ± 0.3	3.2 ± 1.4*	1.1 ± 0.2	1.2 ± 0.4	2.7 ± 1.2*	1.2 ± 0.2
CL_{total} (ml/min/kg)	107 ± 15	76 ± 14*	93 ± 9	N.A.	N.A.	N.A.	N.A.	N.A.	N.A.
V_d (L/kg)	5.5 ± 0.5	13.2 ± 3.9*	4.8 ± 0.6	N.A.	N.A.	N.A.	N.A.	N.A.	N.A.
F (%)	N.A.	N.A.	N.A.	10.0	83.3	25.9	17.8	29.9	16.4
1-OH-THA									
T_{max} (h)	0.3 ± 0.1	0.3 ± 0.1	0.7 ± 0.3*	0.6 ± 0.2	3.3 ± 1.8*#	0.8 ± 0.2#	0.5 ± 0.2	1.5 ± 0.9*	1.6 ± 0.2*
C_{max} (ng/ml)	457 ± 118	515 ± 54	339 ± 51	170 ± 79	460 ± 141*	176 ± 56#	304 ± 35	356 ± 114	265 ± 41
AUC_{0-6h} (ng·h/ml)	808 ± 115	1968 ± 180*	841 ± 175	333 ± 140	2137 ± 647*	482 ± 46#	786 ± 80	1383 ± 496*	758 ± 138
$t_{1/2}$ (h)	1.4 ± 0.2	N.A.	1.4 ± 0.2	1.7 ± 0.6	N.A.	2.0 ± 0.8	2.0 ± 0.9	N.A.	1.8 ± 1.0
2-OH-THA									
T_{max} (h)	0.3 ± 0.1	0.3 ± 0.1	1.0 ± 0.4*	0.5 ± 0.1	4.0 ± 1.7*#	1.8 ± 0.4*	0.6 ± 0.2	1.6 ± 0.9*	1.4 ± 0.2*
C_{max} (ng/ml)	50 ± 14	56 ± 6	35 ± 4	18 ± 8	52 ± 16*	13 ± 4#	33 ± 3	41 ± 14	26 ± 10
AUC_{0-6h} (ng·h/ml)	98 ± 11	217 ± 18*	98 ± 13	41 ± 17	234 ± 64*	45 ± 7#	99 ± 8	169 ± 60*	89 ± 21
$t_{1/2}$ (h)	1.8 ± 0.3	N.A.	1.5 ± 0.2	2.4 ± 0.9	N.A.	2.7 ± 0.9	3.2 ± 2.0	N.A.	3.1 ± 2.1
Metabolic ratio[a]	1.4 ± 0.2	3.0 ± 0.4*	1.3 ± 0.2	6.0 ± 1.2	4.0 ± 1.1*#	3.1 ± 0.8*#	8.8 ± 2.0	9.5 ± 2.4	8.0 ± 2.3

Data are presented as the mean ± s.d. ($n = 5$); *N.A.* not applicable

* $p < 0.05$ for comparison with the conscious model

# $p < 0.05$ for comparison between i.n. group and p.o. group under the same rat model

[a] Overall metabolic ratio, calculated as the sum of metabolic ratios of 1-OH-THA and 2-OH-THA

anesthetized model than that in the short-term anesthetized model. No significant difference was found in the $t_{1/2}$ of both THA metabolites between the short-term anesthetized model and conscious model. Longer T_{max} of the two metabolites were found in the short-term anesthetized model, which might be due to the inhibitory effect of ether anesthesia on CYP 1A-mediated metabolite formation in the early period after ether exposure. Nevertheless, no significant difference was detected in the C_{max} and AUC_{0-6h} between the short-term anesthetized model and conscious model, reflecting the fading out of the ether's inhibitory effect on metabolism (which would be discussed in Discussion). Overall, although there were deviations in the plasma concentration-time profile (e.g. longer time for the metabolites to reach C_{max} in the short-term anesthetized model), systemic exposures (C_{max} and AUC_{0-6h}) of THA and its metabolites and the metabolic ratio in the short-term anesthetized model were comparable to that of the conscious model, both of which were lower than those in the long-term anesthetized model.

i.n. THA

Compared with that in the long-term anesthetized model, the accumulation of plasma THA was less prominent in the short-term anesthetized model (with a 2.8-fold and 3.0-fold increase in C_{max} and AUC_{0-6h} comparing with the conscious model, respectively). Moreover, the T_{max} (0.3 h) and $t_{1/2}$ (1.1 h) of THA in the short-term anesthetized model were almost the same as that in the conscious model.

Regarding the metabolites 1-OH-THA (Fig. 4b) and 2-OH-THA (Fig. 4c), comparable C_{max} and AUC_{0-6h} were obtained in the short-term anesthetized model and conscious model (Table III), which were much lower than that observed in long-term anesthetized model.

In the conscious model, the PK profile of parent THA after i.n. administration was indeed similar to that after p.o. administration (similar T_{max} and $t_{1/2}$), but the bioavailability of i.n. THA (10%) was even lower than that of p.o. THA (17.8%). The low i.n. bioavailability of THA in conscious rats might be due to not only the drainage of drug solution into GI tract, but also the loss of drug solution caused by sneezing

during and after nasal dosing. Such difficulty in accurate drug dosing and low i.n. bioavailability in conscious rat model was also encountered by other research groups (e.g. (3,12)). In addition, the metabolic ratio of i.n. group (6.0) was much higher than that of i.v. group (1.4), but was slightly lower than that of p.o. group (8.8). This further indicated that most of the i.n. THA dose was swallowed by the conscious animal into GI tract, while only a small portion of the nasal dose was absorbed within the nasal cavity and bypassed the first-pass metabolism. Applying short-term anesthesia to rats facilitated the retention and absorption of drug solution inside the nasal cavity, which helped to reduce the amount of swallowed drug (metabolic ratio reduced to 3.1) and increase the i.n. bioavailability to 26%.

p.o. THA

The trends observed after p.o. THA administration were similar to that after i.v. and i.n. THA administrations. In comparison to the conscious model, although the short-term anesthetized model had delayed T_{max} and lower plasma concentrations of both THA and its metabolites at the early period (0–30 min), the C_{max} and AUC_{0-6h} values of these compounds were comparable between these two models, which were lower than that observed in long-term anesthetized model. The delay in intestinal absorption of THA, caused by the inhibitory effect of diethyl ether on gastric emptying and small intestinal transit (41,42), subsequently led to the delayed formation and T_{max} of the THA metabolites. The oral bioavailability (F) and $t_{1/2}$ of THA in the short-term anesthetized model were virtually the same as that in the conscious model, both of which were significantly lower than that in the long-term anesthetized model. This indicates that the short-lasting ether anesthesia did not impose prominent changes in the overall absorption and disposition of THA, while the long-lasting ketamine/xylazine anesthesia could have notable impact on the clearance of THA, leading to overestimation of oral THA bioavailability.

DISCUSSION

Although the long-term anesthetized surgical model described by Hussain in 1980 (2) has been frequently adopted by researchers to compare the nasal delivery efficiency of different candidate compounds or different formulations, the appropriateness of this classic model for PK investigation has not been systematically evaluated. Using LOX and THA as model drugs, the present study for the first time clearly demonstrated that the PK data of the nasal drugs and their metabolites obtained with the long-term anesthetized model differed dramatically from those with normal, non-manipulated conscious model.

Deviation of PK in the Long-Term Anesthesia Model From the Conscious Model

Results from both i.n. LOX and i.n. THA demonstrated that accumulation of the parent drug and its metabolites occurred in the classic long-term anesthetized surgical model in comparison to the conscious model. The factors causing the deviation of PK profile of nasal drug in the long-term anesthetized model from that in the conscious model are discussed as follows.

The long-term anesthetized rats were kept in supine position throughout the experimental period, and the drug solution resided in the nasal cavity and had an intimate contact with the nasal mucosa. In contrast, loss of drug solution during dosing (difficult to dose the moving and struggling animal) and after dosing (due to nasal mucociliary clearance, drainage into GI tract, and expulsion of the drug because of sneezing) could occur in the conscious rat model and, therefore, only a portion of the dose is available for nasal absorption. Thus, the extent of nasal absorption of drug is expected to be much higher in the long-term anesthetized model than that in the conscious model, and the absolute bioavailabilities of nasal drugs obtained with the long-term anesthetized model could be relatively high (approaching 100%) for small lipophilic compounds such as LOX and THA. In addition to nose-to-systemic circulation delivery, the appropriateness of the long-term anesthetized model for nose-to-brain delivery has also been questioned (43) since pooling of the nasal solution in the olfactory region would lead to exaggeration of the nose-to-brain delivery efficiency, which does not occur in conscious rat in a "normal position".

Drug metabolism could be hampered in the long-term anesthetized model. Many anesthetic agents have direct suppressive effects on rat CYP activities (44,45). *In vivo* studies suggested that acute ketamine treatment could moderately inhibit rat hepatic CYP 3A activities by 20−40% for at least 4 to 8 h (9,44,45). In addition, ketamine was also found to shift the metabolic pathway of cocaine from CYP 3A-mediated *N*-desmethylation to methylesterase-mediated hydrolysis in rats (46,47). Since the metabolic conversion of LOX to AMOX is mainly catalyzed by CYP 3A-mediated *N*-desmethylation (25), ketamine might directly inhibit the formation of AMOX. The *N*-desmethylation of 7-OH-LOX to the secondary metabolite 7-OH-AMOX might also be inhibited in the same manner. In both i.n. and i.v. groups, the formations of AMOX and 7-OH-AMOX were suppressed (decreased metabolic ratios of AMOX and 7-OH-AMOX) in the anesthetized model in comparison to the conscious model (Table II). Consequently, the metabolic pathway of LOX shifted from CYP 3A-mediated *N*-desmethylation (25) to CYP 2D-mediated 7-hydroxylation (25), leading to increased formation of 7-OH-LOX in the anesthetized model. Ketamine and xylazine could reduce the amount of unoccupied CYP 3A available for LOX

metabolism since ketamine (48) and xylazine (49) are almost exclusively metabolized by CYP 3A in rat liver. A previous study (40) found that within the first 2 h after a single injection of 80 mg/kg ketamine with 5 mg/kg xylazine to rats, the plasma concentrations of ketamine and xylazine were between $6-13\times10^3$ and 100–200 ng/ml, respectively. Considering that the doses and plasma concentrations of ketamine and xylazine were much higher than those of LOX and they were repeatedly injected to maintain long-term anesthesia, competitive inhibition was likely to contribute to the reduced CYP 3A-mediated AMOX and 7-OH-AMOX formation in the long-term anesthetized model. Ketamine was also found *in vitro* to reduce the rat liver microsomal activity toward CYP 3A substrate by competitive inhibition (44). On the other hand, since THA is mainly metabolized by CYP 1A (50) and ketamine did not alter rat hepatic CYP 1A activities (44,45), the long-term anesthesia should have limited influence on the formation rate of THA metabolites. This was reflected on the formation of THA metabolites in the initial 30 min after i.v. THA administration, since similar PK profiles (enlarged Fig. 3b and c) and T_{max} (Table III) of both 1-OH-THA and 2-OH-THA were obtained between the long-term anesthesia model and the conscious model. Therefore, the accumulation of THA metabolites observed in the long-term anesthetized model should be caused by other mechanisms such as reduction in renal elimination, which could be the rate-limiting step in the systemic disposition of the THA metabolites.

Total hepatic blood flow is usually decreased during anesthesia with various anesthetics including ketamine (51). The majority of the anesthetics decrease portal blood flow in association with a decrease in cardiac output (51). In rats anesthetized with a single injection of ketamine/xylazine, both the heart rate and blood pressure are suppressed by 20−40% (52,53). More importantly, the suppression on cardiovascular function persists for at least 4 h after the ketamine/xylazine injection (40,52). Such reduction in cardiac output might in turn reduce the blood flow to liver and kidney, which receive 17% and 14% of cardiac output, respectively (54). Both LOX and THA are highly extracted drugs (≥70%). Since the hepatic clearance of highly extracted drugs is hepatic blood flow-dependent, anesthesia-induced reduction in hepatic blood flow could have significant impact on the metabolic conversion of both drugs. At 4 h after anesthesia with ketamine/xylazine and surgery in rats, the portal venous blood flow could be lowered by 40% compared with rats 3 days after anesthesia and surgery, which had their portal venous blood flow returned to baseline level (9). The systemic clearance of i.v. midazolam (CYP 3A probe substrate) was also lowered by 40% in rats 4 h after anesthesia and surgery compared with rats 3 days after anesthesia and surgery (9). In the long-term anesthetized model, the systemic clearances of i.v. LOX and i.v. THA were lowered by 40% and 30% respectively, which were consistent with the proposal that anesthesia-induced reduction in hepatic blood flow was the main mechanism behind the suppressed systemic clearance of the parent drugs.

Renal elimination of drug and its metabolites could also be retarded in the long-term anesthetized model. Most of the injectable anesthetics including ketamine could reduce renal blood flow, glomerular filtration rate and urine flow rate in rats (55), even when they are administered at subanesthetic doses (56). The effect of anesthesia on the biodistribution of carboplatin, the major clearance route of which is through urinary excretion, was studied in rats (57). Ketamine/xylazine anesthesia, similar to other injectable anesthetics, increased the accumulation of platinum in both plasma and tissues including the brain, and anesthesia-induced alteration in renal function was suggested to be the reason for the enhanced drug accumulation. Since the CL_{total} of i.v. LOX and THA in the conscious model exceeded the rat hepatic blood flow (60 ml/min/kg (54)), extrahepatic clearance should also be taken into account. Renal clearance is an important route of elimination of THA, LOX and their metabolites in rats. THA is excreted in urine mainly as 1-OH-THA and, to a lesser extent, 2-OH-THA and THA (27). LOX is excreted as glucuronides of the 7-hydroxylated metabolites (26) and as glucuronide of LOX (58). Therefore, ketamine/xylazine might reduce renal clearance of the drugs in the anesthetized model through the following two mechanisms: (i) reduction in renal blood flow leading to reduced glomerular filtration, and (ii) inhibitory effect of ketamine on renal glucuronidation enzymes (59) leading to reduced renal extractions of LOX and its metabolites. Moreover, a study by Yang *et al.* (10) suggested that nasal surgery itself could suppress the systemic clearance of stavudine, a drug that is eliminated from rats mainly by urine as unchanged drug (60), although the underlying mechanism remained to be elucidated. In addition to kidney, extrahepatic clearance might also occur in other organs such as the brain and lung. However, information is limited and the few *in vitro* studies could not identify any metabolite formation when THA was incubated with rat brain homogenate (61) or when LOX was incubated with human lung microsomes (62). Therefore, kidney could be the major organ responsible for the extrahepatic clearance of the two drugs.

The possibility of nasal metabolism (16) cannot be excluded. Phase I enzymes such as CYPs and conjugative Phase II enzymes such as UDP-glucuronyltransferases have been identified in both the nasal respiratory mucosa (63) and olfactory mucosa (64) of rats. Both qualitative and quantitative differences exist between nasal mucosa and liver in terms of CYP expression. In rats, some isoforms are expressed in olfactory mucosa but not in the liver (e.g. CYP 1A1), whereas some isoforms (e.g. CYPs 2D2, 3A1 and 3A2) are expressed only in liver (65). An *in vitro* study found that the affinity (K_m) of rat olfactory mucosa microsomes toward phenacetin (metabolized mainly by CYPs 1A1 and 1A2) were about 10 times higher than that of rat liver microsomes, whereas V_{max}

confirmed the high activity of olfactory mucosa toward this substrate in comparison to the liver (V_{max} 4-fold higher in olfactory mucosa microsomes) (65). It is possible that in addition to swallowing of THA into GI tract, CYP 1A-mediated THA metabolism at the nasal mucosa also contributed to the relatively high metabolic ratio (6.0) in the i.n. conscious model. In contrast, exposure to ether might inhibit CYP 1A activities (66) of the nasal mucosa, which in turn lowered the metabolic ratio (3.1) in the i.n. short-term anesthetized model.

The potential effect of anesthesia on drug plasma protein binding is considered. Although the percentage of LOX bound to plasma protein is uncertain, its metabolite AMOX shows high protein binding (~90% in human plasma) (67), and their affinities to the plasma protein α_1-acid glycoprotein are at least comparable to that of propranolol (>70% bound to α_1-acid glycoprotein) (68,69). THA and 1-OH-THA are moderately bound to plasma protein (~60%) but they are only weakly bound to α_1-acid glycoprotein (70–72). On the other hand, both the plasma protein binding and α_1-acid glycoprotein binding of ketamine are in the range of 20−40% (73) and independent of ketamine concentrations (74). Therefore, based on the capacity and concentration independency of ketamine plasma protein binding (75), it is not likely that it would displace LOX, THA or their metabolites from the plasma protein to increase their plasma unbound fraction.

The PK differences between different rat models were route-dependent. For instance, the $AUC_{0-\infty}$ of LOX and THA increased by around 80% and 40%, respectively, in the long-term anesthetized model compared with the conscious model after i.v. drug administrations, whereas the $AUC_{0-\infty}$ increased by around 280% and 1100%, respectively, in the long-term anesthetized model after i.n. drug administrations. On the other hand, the exact effects of long-term anesthesia on drug bioavailability were difficult to judge after p.o. drug administration since the absorption of drug in GI tract was severely retarded and was not yet finished, and a complete PK profile might not be obtained within the experimental period. Therefore, accurate determination of the absolute bioavailability ($AUC_{i.n.}$ *vs* $AUC_{i.v.}$) or the relative bioavailability ($AUC_{i.n.}$ *vs* $AUC_{p.o.}$) of a nasal drug still could not be achieved even if long-term anesthesia had been applied to all the administration groups.

Potential Advantages of the Short-Term Anesthetized Model

Since the physiological conditions of the animals in the classic model (long-term anesthetized with nasal surgery) are quite different from that in the actually clinical practice, transiently sedated rats (short-term anesthetized) without nasal surgery were also employed in several studies to investigate the absorption and PK of nasal drugs (12,76,77). To induce short-term anesthesia, inhalation anesthetic agents like diethyl ether, halothane, or isoflurane are applied for a few minutes to immobilize the animal which facilitates the nasal drug administration, and the animal is allowed to recover from anesthesia and regain consciousness within a short period (e.g. several minutes). The potential advantages of the short-term anesthetized model for nasal delivery studies are discussed as follows.

The PK parameters of i.n., i.v., and p.o. THA obtained with the conscious model were much more comparable to that obtained with the short-term anesthetized model than those obtained with the long-term anesthetized model. Liu *et al.* (66) found that although the activities of CYP 1A and CYP 2B in liver and kidney were inhibited by 20 to 70% after 6 min of diethyl ether exposure to rats, their activities in most cases could restore to normal level within 30 to 120 min. In addition, the inhibition of CYP activities by diethyl ether depends on the exposure period. The shorter the period of exposure, the less inhibitory effect it will have on the CYP activities and the faster the activities recover (78–80). In the present study, 3 min of diethyl ether exposure (half of that applied by Liu *et al.* (66)) was applied to induce anesthesia, and the rats could recover from anesthesia (with obvious struggling to right themselves) within 4–7 min. Although 2 min of diethyl ether exposure was sufficient to abolish the righting reflex, accurate nasal dosing could not be achieved since sneezing of the administered nasal dose still existed in most of the rats.

For the initial 15 min after i.v. THA administration, the amounts of metabolites (i.e. 1-OH-THA and 2-OH-THA) generated in the short-term anesthetized model was significantly lower than that in the conscious model (enlarged figures of Fig. 3b and c), which could be attributed to the suppressed CYP activities after diethyl ether anesthesia. However, the elimination phases of THA and its metabolites (from 1 to 6 h) after i.v. THA administrations in the short-term anesthetized model were similar to that in the conscious model with no significant difference in $t_{1/2}$ and CL_{total} (Fig. 3, Table III), which indicated that the activities of CYP-mediated metabolism had recovered to normal level. This is consistent with a previous report that an exposure of 5 to 10 min of diethyl ether did not affect the overall plasma clearances of the four probe substrates of CYPs 1A, 2B/2C, 2D1 and 3A in rats (45). The initial inhibition of metabolic enzymes by diethyl ether led to longer T_{max} of THA metabolites. However, the AUC values of THA, 1-OH-THA and 2-OH-THA obtained in the short-term anesthetized model were similar to that obtained in the conscious model, but were significantly higher in the long-term anesthetized model (Table III). The absolute bioavailability of i.n. THA in the short-term anesthetized model (26%) was much closer to that in the conscious model (10%) than to that in the long-term anesthetized model (83%), reflecting the close resemblance of the short-term anesthetized model to the conscious model. Moreover, inhalation anesthetics tend to have fewer cardiovascular and hemodynamic effects in rodents than the injectable anesthetics (81,82). While

ketamine/xylazine anesthesia induces severe cardiovascular depression (83) which could, in turn, reduce blood flow to organs responsible for elimination of drugs and their metabolites (i.e. liver and kidney as discussed above), the influences on organ perfusion are expected to be smaller in animals anesthetized temporarily with inhalation anesthetics although the influences depend on the anesthetic applied (84).

In summary, the PK of nasal drug obtained with anesthetized rat models differ from that with conscious rat model due to altered absorption, metabolism and elimination processes. The long-term anesthesia and invasive nasal surgery applied to the classic rat model (2) could severely retard the systemic elimination of the nasal drug and its metabolites, leading to overestimation of the nasal bioavailability. The short-term anesthetized model, on the other hand, seems to be more suitable than the long-term anesthetized model for nasal PK study since the impact on drug PK is smaller and temporary while accurate nasal dosing could still be achieved. The invasive nasal surgery is avoided, which enables higher throughput and makes the short-term anesthetized model more physiologically plausible since the surgical trauma and repeated anesthesia imposed to the animals could interfere with the outcomes of PK and pharmacodynamic assessments. The animals are allowed to recover for further assessments over a prolonged period of time in the short-term anesthetized model, whereas the duration of experiment is at most 4 to 6 h in the long-term anesthetized model due to the tremendous stress caused by repeated anesthesia and nasal surgery, making it an unsuitable model for PK investigations of drugs with relatively long half-lives (e.g. $t_{1/2}$ >2–4 h).

CONCLUSION

For nasal drug delivery studies, PK data obtained from anesthetized rats must be analyzed with caution since anesthesia could have profound impacts on the drug PK processes, and the impacts depend on the rat model adopted. Accumulations of the drug and its metabolites were prominent in the long-term anesthetized model since their systemic eliminations were severely retarded. In contrast, PK data obtained with the short-term anesthetized non-surgical model resembled that with the conscious model. While the use of anesthesia is necessitated for accurate nasal dosing to rats, the short-term anesthetized model might be a better model than the classic long-term anesthetized model in the PK investigation of nasal drug delivery.

ACKNOWLEDGMENTS AND DISCLOSURES

Yin Cheong Wong and Shuai Qian made equal contributions to this work. This work was funded by CUHK Direct Grant 4450272 and General Research Fund CUHK 480809. The authors are grateful to Ms. Sophia Yui Kau Fong for her valuable suggestions to the manuscript.

REFERENCES

1. Illum L. Nasal delivery. The use of animal models to predict performance in man. J Drug Target. 1996;3(6):427–42.
2. Hussain A, Hirai S, Bawarshi R. Nasal absorption of propranolol from different dosage forms by rats and dogs. J Pharm Sci. 1980;69(12):1411–13.
3. Daugherty AL, Liggitt HD, Mccabe JG, Moore JA, Patton JS. Absorption of recombinant methionyl-human growth hormone (Met-hGH) from rat nasal mucosa. Int J Pharm. 1988;45(3):197–206.
4. Schipper NGM, Hermens WAJJ, Romeyn SG, Verhoef J, Merkus FWHM. Nasal absorption of 17-beta-estradiol and progesterone from a dimethyl-cyclodextrin inclusion formulation in rats. Int J Pharm. 1990;64(1):61–6.
5. Kao HD, Traboulsi A, Itoh S, Dittert L, Hussain A. Enhancement of the systemic and CNS specific delivery of L-dopa by the nasal administration of its water soluble prodrugs. Pharm Res. 2000;17(8):978–84.
6. Naguib M, Magboul MMA, Jaroudi R. Clinically significant drug interactions with general anaesthetics—Incidence, mechanisms and management. CNS Drugs. 1997;8(1):51–78.
7. Moench PA, Heran CL, Stetsko PI, Mathias NR, Wall DA, Hussain MA, *et al.* The effect of anesthesia on the pharmacokinetics of sublingually administered verapamil in rabbits. J Pharm Sci. 2003;92(9):1735–8.
8. Kennedy JM, Van Riji AM. Effects of surgery on the pharmacokinetic parameters of drugs. Clin Pharmacokinet. 1998;35(4):293–312.
9. Uhing MR, Beno DWA, Jiyamapa-Serna VA, Chen Y, Galinsky RE, Hall SD, *et al.* The effect of anesthesia and surgery on CYP3A activity in rats. Drug Metab Dispos. 2004;32(11):1325–30.
10. Yang Z, Huang Y, Gan G, Sawchuk RJ. Microdialysis evaluation of the brain distribution of stavudine following intranasal and intravenous administration to rats. J Pharm Sci. 2005;94(7):1577–88.
11. Gozes I, Bardea A, Reshef A, Zamostiano R, Zhukovsky S, Rubinraut S, *et al.* Neuroprotective strategy for Alzheimer disease: intranasal administration of a fatty neuropeptide. Proc Natl Acad Sci U S A. 1996;93(1):427–32.
12. Mayor SH, Illum L. Investigation of the effect of anaesthesia on nasal absorption of insulin in rats. Int J Pharm. 1997;149(1):123–9.
13. Hanson LR, Roeytenberg A, Martinez PM, Coppes VG, Sweet DC, Rao RJ, *et al.* Intranasal deferoxamine provides increased brain exposure and significant protection in rat ischemic stroke. J Pharmacol Exp Ther. 2009;330(3):679–86.
14. Tse FLS, Nickerson DF, Aun R. Effect of isoflurane anesthesia on antipyrine pharmacokinetics in the rat. Pharm Res. 1992;9(11):1515–17.
15. Gantenbein M, Abat C, Attolini L, Pisano P, Emperaire N, Bruguerolle B. Ketamine effects on bupivacaine local anaesthetic activity and pharmacokinetics of bupivacaine in mice. Life Sci. 1997;61(20):2027–33.
16. Wong YC, Zuo Z. Intranasal delivery-modification of drug metabolism and brain disposition. Pharm Res. 2010;27(7):1208–23.
17. Wong YC, Qian S, Zuo Z. Regioselective biotransformation of CNS drugs and its clinical impact on adverse drug reactions. Expert Opin Drug Metab Toxicol. 2012;8(7):833–54.
18. Wong YC, Zuo Z. Preliminary screening of antipsychotic drug candidates for intranasal delivery potentials. 2010 AAPS Annual Meeting and Exposition. New Orleans, LA, USA; 2010, Nov 14–18.
19. Qian S, Mak M, He L, Ho CY, Han Y, Zuo Z. In vitro anti-antiacetylcholinesterase activities and permeabilities of novel potential

anti-Alzheimer's agents. 9th International Society for the Study of Xenobiotics (ISSX) Meeting. Istanbul, Turkey; 2010, Sep 04-08.
20. Wang S, Chow MS, Zuo Z. An approach for rapid development of nasal delivery of analgesics–identification of relevant features, in vitro screening and in vivo verification. Int J Pharm. 2011;420(1):43–50.
21. Midha KK, Rawson MJ, Hubbard JW. The role of metabolites in bioequivalence. Pharm Res. 2004;21(8):1331–44.
22. Wong YC, Wo SK, Zuo Z. Investigation of the disposition of loxapine, amoxapine and their hydroxylated metabolites in different brain regions, CSF and plasma of rat by LC-MS/MS. J Pharm Biomed Anal. 2012;58:83–93.
23. Kukan M, Bezek S, Pool WF, Woolf TF. Metabolic disposition of tacrine in primary suspensions of rat hepatocyte and in single-pass perfused liver: in vitro/in vivo comparisons. Xenobiotica. 1994;24(11):1107–17.
24. Qian S, Wo SK, Zuo Z. Pharmacokinetics and brain dispositions of tacrine and its major bioactive monohydroxylated metabolites in rats. J Pharm Biomed Anal. 2012;61:57–63.
25. Luo JP, Vashishtha SC, Hawes EM, Mckay G, Midha KK, Fang J. In vitro identification of the human cytochrome p450 enzymes involved in the oxidative metabolism of loxapine. Biopharm Drug Dispos. 2011;32(7):398–407.
26. Narige T, Mizumura M, Okuizumi N, Matsumoto K, Furukawa Y, Hondo T. Study of the absorption, distribution, metabolism, and excretion of amoxapine in rats. Yakuri Chiryo. 1981;9(5):1885–92.
27. Pool WF, Reily MD, Bjorge SM, Woolf TF. Metabolic disposition of the cognition activator tacrine in rats, dogs, and humans. Species comparisons. Drug Metab Dispos. 1997;25(5):590–7.
28. Marks DR, Tucker K, Cavallin MA, Mast TG, Fadool DA. Awake intranasal insulin delivery modifies protein complexes and alters memory, anxiety, and olfactory behaviors. J Neurosci. 2009;29(20):6734–51.
29. Lutz JD, Isoherranen N. Prediction of relative in vivo metabolite exposure from in vitro data using two model drugs: dextromethorphan and omeprazole. Drug Metab Dispos. 2012;40(1):159–68.
30. Han S, Zhang J, Tang J. Effects of compound ketamine oral solution on gastrointestinal motility in rats. World China J Digestol. 2010;18(23):2405–9.
31. Hsu WH. Xylazine-induced delay of small intestinal transit in mice. Eur J Pharmacol. 1982;83(1–2):55–60.
32. Yuasa H, Matsuda K, Watanabe J. Influence of anesthetic regimens on intestinal absorption in rats. Pharm Res. 1993;10(6):884–8.
33. Dahan A, Mendelman A, Amsili S, Ezov N, Hoffman A. The effect of general anesthesia on the intestinal lymphatic transport of lipophilic drugs: Comparison between anesthetized and freely moving conscious rat models. Eur J Pharm Sci. 2007;32(4–5):367–74.
34. van de Kerkhof EG, de Graaf IA, Groothuis GM. In vitro methods to study intestinal drug metabolism. Curr Drug Metab. 2007;8(7):658–75.
35. FDA Guidence. Estimating the maximum safe starting dose in initial clinical trials for therapeutics in adult healthy volunteers. In. Rockville, MD, USA; 2005.
36. Spyker DA, Munzar P, Cassella JV. Pharmacokinetics of loxapine following inhalation of a thermally generated aerosol in healthy volunteers. J Clin Pharmacol. 2010;50(2):169–79.
37. Hirai S, Yashiki T, Matsuzawa T, Mima H. Absorption of drugs from the nasal mucosa of rat. Int J Pharm. 1981;7(4):317–25.
38. Hussain MA, Knabb R, Aungst BJ, Kettner C. Anticoagulant activity of a peptide boronic acid thrombin inhibitor by various routes of administration in rats. Peptides. 1991;12(5):1153–4.
39. Donovan MD, Flynn GL, Amidon GL. Absorption of polyethylene glycols 600 through 2000: the molecular weight dependence of gastrointestinal and nasal absorption. Pharm Res. 1990;7(8):863–8.
40. Veilleux-Lemieux D, Beaudry F, Hélie P, Vachon P. Effects of endotoxemia on the pharmacodynamics and pharmacokinetics of ketamine and xylazine anesthesia in Sprague–Dawley rats. Vet Med Res Rep. 2012;3:99–109.
41. Miller GH. The effects of general anesthesia on the musculat activity of the gastrointestinal tract a study of ether, chloroform, ethylene and nitrous-oxide. J Pharmacol Exp Ther. 1926;27(1):41–59.
42. Reynell PC, Spray GH. The effect of ether and pentobarbitone sodium on gastrointestinal function in the intact rat. Br J Pharmacol Chemother. 1957;12(1):104–6.
43. Charlton ST, Davis SS, Illum L. Nasal administration of an angiotensin antagonist in the rat model: effect of bioadhesive formulations on the distribution of drugs to the systemic and central nervous systems. Int J Pharm. 2007;338(1–2):94–103.
44. Meneguz A, Fortuna S, Lorenzini P, Volpe MT. Influence of urethane and ketamine on rat hepatic cytochrome P450 in vivo. Exp Toxicol Pathol. 1999;51(4–5):392–6.
45. Loch JM, Potter J, Bachmann KA. The influence of anesthetic agents on rat hepatic cytochromes P450 in vivo. Pharmacology. 1995;50(3):146–53.
46. Rofael HZ, Abdel-Rahman MS. The role of ketamine on plasma cocaine pharmacokinetics in rat. Toxicol Lett. 2002;129(1–2):167–76.
47. Rofael HZ, Abdell-Rahman MS. Reduction of tissue concentration of cocaine in rat by ketamine. J Toxicol Environ Health A. 2003;66(3):241–51.
48. Shaw AA, Hall SD, Franklin MR, Galinsky RE. The influence of L-glutamine on the depression of hepatic cytochrome P450 activity in male rats caused by total parenteral nutrition. Drug Metab Dispos. 2002;30(2):177–82.
49. Lavoie DSG, Pailleux F, Vachon P, Beaudry F. Characterization of xylazine metabolism in rat liver microsomes using liquid chromatography-hybrid triple quadrupole-linear ion trap-mass spectrometry. Biomed Chromatogr. 2013;27(7):882–8.
50. Spaldin V, Madden S, Adams DA, Edwards RJ, Davies DS, Park BK. Determination of human hepatic cytochrome P4501A2 activity in vitro use of tacrine as an isoenzyme-specific probe. Drug Metab Dispos. 1995;23(9):929–34.
51. Gelman S. General anesthesia and hepatic circulation. Can J Physiol Pharmacol. 1987;65(8):1762–79.
52. Picollo C, Serra AJ, Levy RF, Antonio EL, Santos LD, Tucci PJF. Hemodynamic and thermoregulatory effects of xylazine-ketamine mixture persist even after the anesthetic stage in rats. Arq Bras Med Vet Zootec. 2012;64:860–4.
53. Rodrigues SF, de Oliveira MA, Martins JO, Sannomiya P, de Cássia TR, Nigro D, *et al.* Differential effects of chloral hydrate- and ketamine/xylazine-induced anesthesia by the s.c. route. Life Sci. 2006;79(17):1630–7.
54. Brown RP, Delp MD, Lindstedt SL, Rhomberg LR, Beliles RP. Physiological parameter values for physiologically based pharmacokinetic models. Toxicol Ind Health. 1997;13(4):407–84.
55. Gumbleton M, Nicholls PJ, Taylor G. Differential-effects of anesthetic regimens on gentamicin pharmacokinetics in the rat - a comparison with chronically catheterized conscious animals. Pharm Res. 1990;7(1):41–5.
56. Petersen JS, Shalmi M, Christensen S, Haugan K, Lomholt N. Comparison of the renal effects of six sedating agents in rats. Physiol Behav. 1996;60(3):759–65.
57. Sancho AR, Dowell JA, Wolf W. The effects of anesthesia on the biodistribution of drugs in rats: a carboplatin study. Cancer Chemother Pharmacol. 1997;40(6):521–5.
58. Cooper TB, Kelly RG. GLC analysis of loxapine, amoxapine, and their metabolites in serum and urine. J Pharm Sci. 1979;68(2):216–19.
59. Qi X, Evans AM, Wang JP, Miners JO, Upton RN, Milne RW. Inhibition of morphine metabolism by ketamine. Drug Metab Dispos. 2010;38(5):728–31.
60. Kaul S, Dandekar KA, Schilling BE, Barbhaiya RH. Toxicokinetics of 2′,3′-didehydro-3′-deoxythymidine, stavudine (D4T). Drug Metab Dispos. 1999;27(1):1–12.
61. McNally WP, Pool WF, Sinz MW, Dehart P, Ortwine DF, Huang CC, *et al.* Distribution of tacrine and metabolites in rat brain and

plasma after single- and multiple-dose regimens. Evidence for accumulation of tacrine in brain tissue. Drug Metab Dispos. 1996;24(6):628–33.
62. Huie K, Reed A, Takahashi L, Cassella J. Characterization of loxapine human metabolism. Drug Metab Rev. 2008;40:210–11.
63. Thornton-Manning JR, Dahl AR. Metabolic capacity of nasal tissue interspecies comparisons of xenobiotic-metabolizing enzymes. Mutat Res. 1997;380(1–2):43–59.
64. Heydel JM, Coelho A, Thiebaud N, Legendre A, Le Bon AM, Faure P, *et al.* Odorant-binding proteins and xenobiotic metabolizing enzymes: implications in olfactory perireceptor events. Anat Rec (Hoboken). 2013;296(9):1333–45.
65. Minn AL, Pelczar H, Denizot C, Martinet M, Heydel JM, Walther B, *et al.* Characterization of microsomal cytochrome P450-dependent monooxygenases in the rat olfactory mucosa. Drug Metab Dispos. 2005;33(8):1229–37.
66. Liu PT, Ioannides C, Shavila J, Symons AM, Parke DV. Effects of ether anaesthesia and fasting on various cytochromes P450 of rat liver and kidney. Biochem Pharmacol. 1993;45(4):871–7.
67. Mazzola CD, Miron S, Jenkins AJ. Loxapine intoxication: case report and literature review. J Anal Toxicol. 2000;24(7):638–41.
68. Ferry DG, Caplan NB, Cubeddu LX. Interaction between antidepressants and alpha1-adrenergic receptor antagonists on the binding to alpha1-acid glycoprotein. J Pharm Sci. 1986;75(2):146–9.
69. Urien S, Bree F, Testa B, Tillement JP. pH-dependency of basic ligand binding to alpha 1-acid glycoprotein (orosomucoid). Biochem J. 1991;280:277–80.
70. Telting-Diaz M, Lunte CE. Distribution of tacrine across the blood–brain barrier in awake, freely moving rats using in vivo microdialysis sampling. Pharm Res. 1993;10(1):44–8.
71. Makela PM, Truman CA, Ford JM, Roberts CJ. Characteristics of plasma protein binding of tacrine hydrochloride: a new drug for Alzheimer's disease. Eur J Clin Pharmacol. 1994;47(2):151–5.
72. Wood DM, Ford JM, Roberts CJ. Variability in the plasma protein binding of velnacrine (1-hydroxy tacrine hydrochloride). A potential agent for Alzheimer's disease. Eur J Clin Pharmacol. 1996;50(1–2):115–19.
73. Dayton PG, Stiller RL, Cook DR, Perel JM. The binding of ketamine to plasma proteins: emphasis on human plasma. Eur J Clin Pharmacol. 1983;24(6):825–31.
74. Hijazi Y, Boulieu R. Protein binding of ketamine and its active metabolites to human serum. Eur J Clin Pharmacol. 2002;58(1):37–40.
75. Wood M. Plasma drug binding: implications for anesthesiologists. Anesth Analg. 1986;65(7):786–804.
76. Dyer AM, Hinchcliffe M, Watts P, Castile J, Jabbal-Gill I, Nankervis R, *et al.* Nasal delivery of insulin using novel chitosan based formulations: a comparative study in two animal models between simple chitosan formulations and chitosan nanoparticles. Pharm Res. 2002;19(7):998–1008.
77. Zhao Y, Tao T, Wu J, Pi J, He N, Chai X, *et al.* Pharmacokinetics of tramadol in rat plasma and cerebrospinal fluid after intranasal administration. J Pharm Pharmacol. 2008;60(9):1149–54.
78. Liu PT, Kentish PA, Symons AM, Parke DV. The effects of ether anaesthesia on oxidative stress in rats–dose response. Toxicology. 1993;80(1):37–49.
79. Plate AY, Crankshaw DL, Gallaher DD. The effect of anesthesia by diethyl ether or isoflurane on activity of cytochrome P450 2E1 and P450 reductases in rat liver. Anesth Analg. 2005;101(4):1063–4.
80. Ida S, Yokota M, Yoshioka H, Takiguchi Y. Single exposure to gasoline or ether reduces cytochrome P-450 activities without affecting UDP-glucuronosyltransferase activity in rat liver. J Occup Health. 2000;42(2):84–5.
81. Janssen BJA, De Celle T, Debets JJM, Brouns AE, Callahan MF, Smith TL. Effects of anesthetics on systemic hemodynamics in mice. Am J Physiol Heart Circ Physiol. 2004;287(4):H1618–24.
82. Chaves AA, Weinstein DM, Bauer JA. Non-invasive echocardiographic studies in mice - influence of anesthetic regimen. Life Sci. 2001;69(2):213–22.
83. Buitrago S, Martin TE, Tetens-Woodring J, Belicha-Villanueva A, Wilding GE. Safety and efficacy of various combinations of injectable anesthetics in BALB/c mice. J Am Assoc Lab Anim Sci. 2008;47(1):11–7.
84. Seyde WC, Longnecker DE. Anesthetic influences on regional hemodynamics in normal and hemorrhaged rats. Anesthesiology. 1984;61(6):686–98.